JOURNAL OF Materials CHEMISTRY

Molecular rectification: characterisation of a dye sandwiched between gold electrodes

Geoffrey J. Ashwell,* Daniel S. Gandolfo and Richard Hamilton

The Nanomaterials Group, Centre for Photonics and Optical Engineering, The Whittle Building, Cranfield University, Cranfield, UK MK43 0AL. E-mail: g.j.ashwell@cranfield.ac.uk

Received 19th November 2001, Accepted 4th January 2002
First published as an Advance Article on the web 28th January 2002

Langmuir–Blodgett (LB) films of the dye, 4-{2-[4-(*N*,*N*-dibutylaminophenyl]vinyl}-*N*-octadecylquinolinium octadecyl sulfate, are non-centrosymmetric and exhibit quadratic enhancement of the second-harmonic intensity with the number of layers when corrected for absorbance. The optimum effective susceptibility at 1.064 μm, monolayer thickness and refractive indices at the fundamental and harmonic frequencies are $\chi^{(2)}_{\text{eff}}$ = 80 pm V^{-1}, $d = 2.46 \pm 0.05$ nm, $n^{\omega} = 1.51 \pm 0.02$ and $n^{2\omega} = 1.65 \pm 0.02$ respectively. In addition, metal/(LB film)/metal devices of the dye exhibit asymmetric current–voltage characteristics and, under forward bias, the current increases exponentially with the electric field. The behaviour is attributed to molecular rectification, the assignment being unambiguous for oxide-free gold electrodes.

Introduction

There have been only four reported molecular rectifiers[1–4] since the seminal publication of Aviram and Ratner,[5] which suggested that bridged donor–acceptor molecules are organic counterparts of the pn junction. The first example, *Z*-β-(*N*-hexadecylquinolinium-4-yl)-α-cyano-4-styryldicyanomethanide, was synthesised as part of Cranfield's nonlinear optics programme[6] and then shown by Sambles and co-workers[1] to exhibit asymmetric current–voltage characteristics. The top electrode was initially restricted to low-sublimation temperature metals to prevent shorting: *e.g.* magnesium[1] and aluminium,[7] the former being silver-coated to limit oxidation. However, the rectification has since been verified by using non-oxidisable gold electrodes.[8,9] The second example, 3,5-dinitrobenzyl 7-(1-oxohexylamino)pyren-2-ylcarbamate,[2] gave improved rectification but the film was sandwiched between silver and silver-coated magnesium and, although probably attributable to molecular rectification, the behaviour cannot be unambiguously assigned. The third and fourth examples,[3,4] octadecyl and dodecyl analogues of a cationic donor–(π-bridge)–acceptor dye, 5-[4-(*N*,*N*-dibutylamino)benzylidene]-2-alkyl-5,6,7,8-tetrahydroisoquinolinium octadecyl sulfate, were investigated as films sandwiched between gold electrodes. The different alkyl groups cause the negatively charged group of the amphiphilic counterion to locate at opposite ends of the chromophore and the polarity for rectification to be reversed. This may be explained by the molecule existing as $D–\pi–A^+$ when the sulfate group is to the right, *i.e.* adjacent to A^+, and as $D^+=\pi=A$ when to the left.[4] Such dipole reversal has been verified by the second-harmonic intensity being cancelled in non-centrosymmetric films of the two forms. It has also been confirmed theoretically. MNDO, AM1 and PM3 calculations have shown a significant dependence of the bond alternation and charge distribution on the location of the counterion with the dimensions being consistent with the aromatic and quinonoid forms of the dye.[4]

In this work we report molecular rectification by LB films of a related cationic dye, 4-{2-[4-(*N*,*N*-dibutylamino)phenyl]-vinyl}-*N*-octadecylquinolinium octadecyl sulfate, and confirm that the molecules are appropriately aligned by investigating both the current–voltage characteristics and second-order nonlinear optical behaviour of the same film. The synthesis of the dye and film characterisation by quartz crystal microbalance (QCM), surface plasmon resonance (SPR) and second-harmonic generation (SHG) studies are reported.

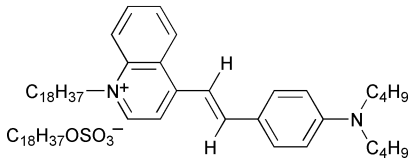

Experimental

To a solution of *N*-octadecyl-4-methylquinolinium iodide (0.52 g, 1 mmol) and *N*,*N*-dibutylaminobenzaldehyde (0.23 g, 1 mmol) in methanol (20 cm^3) was added piperidine (0.1 cm^3) and the mixture heated at reflux for 24 h. The resultant purple precipitate was purified by column chromatography on silica gel eluting with chloroform–methanol (5 : 1, v/v) to afford 4-{2-[4-(*N*,*N*-dibutylamino)phenyl]vinyl}-*N*-octadecylquinolinium iodide: yield, 34%; mp 106–108 °C. Found: C, 69.7; H, 9.0; N, 3.5%. $C_{43}H_{67}N_2I$ requires: C, 69.90; H, 9.14; N, 3.79%. ^{1}H NMR ($CDCl_3$, 200 MHz, *J*/Hz): δ_H 0.90 (t, *J* 6.4, 3H, CH_3), 1.03 (t, *J* 7.0, 6H, CH_3), 1.25 (br s, 30H, CH_2), 1.40–1.47 (m, 4H, CH_2), 1.53–1.68 (m, 4H, CH_2), 2.06 (quintet, *J* 6.8, 2H, $CH_2CH_2N^+$), 3.42 (t, *J* 7.6, 4H, NCH_2), 4.98 (t, *J* 7.2, 2H, CH_2N^+), 6.73 (d, *J* 9.1, 2H, Ar-H), 7.61 (d, *J* 15.5, 1H, C=C-H), 7.68 (d, *J* 9.1, 2H, Ar-H), 7.85–7.89 (m, 1H, Qn-H), 7.96 (d, *J* 15.5, 1H, C=C-H), 8.05–8.12 (m, 2H, Qn-H), 8.26 (d, *J* 6.7, 1H, Qn-H), 8.59 (d, *J* 8.5, 1H, Qn-H), 9.88 (d, *J* 6.8, 1H, Qn-H). *m*/*z* (FAB): 612, 100% $[M + H - I^-]^+$.

The iodide salt of the dye (in chloroform) and sodium octadecyl sulfate (in methanol) were spread, in a 1 : 1 mole ratio, onto the pure water subphase of an LB trough. The Na^+ and I^- ions dissolved, leaving the amphiphilic species at the air–water interface which form an organised monolayer when compressed at 0.5 cm^2 s^{-1}. The floating monolayer was deposited on the upstroke at a surface pressure of 30 mN m^{-1} and a rate of 5 mm min^{-1} for each of the following substrates: 10 MHz quartz crystals for QCM studies; gold-coated BK7 glass for SPR and current–voltage investigations and hydrophilically treated glass for SHG.

 DOI: 10.1039/b110591b

Results and discussion

Structural integrity

The pressure–area (π–A) isotherm exhibits three distinct features: a low-pressure regime where the hydrophilic chromophore is initially parallel to the surface; a broad transition indicating a change in molecular orientation; a steep high-pressure regime where the molecules are upright. The films show variable behaviour in the high-pressure region and, if rapidly compressed, form bilayer arrangements as indicated by the π–A curve of Fig. 1. This results in a mean area of 0.2 nm^2 $molecule^{-1}$ at 55 mN m^{-1} compared with 0.4 nm^2 for the van der Waals cross-section of the two octadecyl groups. Nonetheless, the bilayer can retain the structural integrity of the monolayer and, when deposited, occasionally exhibits a fourfold enhancement of the second-harmonic intensity. However, the remainder of this work concerns the deposition of monolayers rather than bilayers and these may be stabilised by carefully compressing the film at 0.5 cm^2 s^{-1}. It causes the steep high-pressure region to originate at *ca.* 0.6 nm^2 $molecule^{-1}$, as indicated by the inflection in the interconnecting region of Fig. 1, rather than 0.3 nm^2 $molecule^{-1}$. The π–A curve is then consistent with the molecular cross-section and the calculated contact areas in the figure indicate this.

The molecular area in contact with the substrate has been monitored from the frequency change of a 10 MHz quartz crystal, the value being derived using the Sauerbrey equation:[10]

$$A = -4F_o^2 M/\Delta F(\rho\mu)^{1/2}L \quad (1)$$

where F_o and ΔF correspond to the resonance frequency and frequency change respectively, ρ to the density of quartz (2.648 Mg m^{-3}), μ the shear modulus (2.947 $\times$ 10^7 Mg m^{-1} s^{-2}), and M and L to the molecular mass and the Avogadro constant respectively. The derived areas from the QCM study follow the general trend of the isotherm and, in the high-pressure region, are consistent with the estimated molecular cross-section. In this upper region, $\pi \geqslant 40$ mN m^{-1}, the frequency change is typically 170 $\pm$ 20 Hz which corresponds to a molecular footprint of 41 $\pm$ 5 nm^2. However, when compressed or deposited at rates higher than optimum, the frequency doubles and this is indicative of bilayer formation.

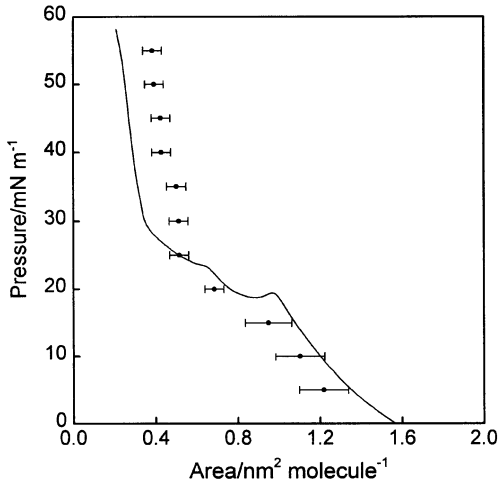

Fig. 1 Pressure *vs.* area isotherm (solid line) showing non-ideal behaviour in the high-pressure regime, the reduced area corresponding to bilayer formation. Monolayer formation is achieved at lower compression rates and the individual data points, which reflect areas in contact with the substrate from a Sauerbrey analysis of the QCM data, were obtained for a monolayer compressed at 0.5 cm^2 s^{-1}. In this case, areas in the high-pressure regime correspond to the sum of molecular cross-sections of the octadecyl chains of the amphiphilic anion and cation.

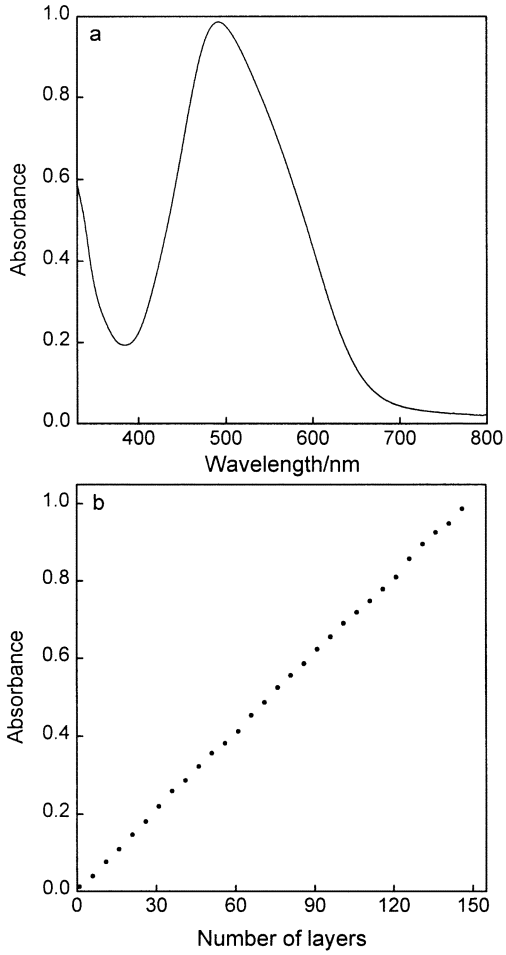

Fig. 2 Spectroscopic data: (a) spectrum of a 150 layer LB film; (b) absorbance *vs.* number of LB layers.

Film characterisation

The deposited film exhibits a broad visible range absorption band at *ca.* 500 nm (Fig. 2) and has excellent layer-by-layer deposition characteristics as indicated by a linear increase of the absorbance with the number of passes through the floating monolayer. In common with other dyes in this series,[4,11] the transition is asymmetric and may be explained by two overlapping bands with absorption maxima at 480 and 560 nm.

The thickness and dielectric permittivities of the LB films were obtained from SPR studies. These were performed on glass/Au/monolayer structures using a Kretschmann configuration[12] and p-polarised monochromatic radiation at the following excitatory wavelengths: 1064 nm (Nd : YAG); 632.8, 611.9, 604.0, 594.1 and 543.5 nm (multiline HeNe); 532.0 nm (frequency-doubled Nd : YAG). The attenuated total reflection was measured before and after deposition and the data analysed by one and two-layer models respectively using Fresnel reflection formulae. Analysis provided a thickness of 2.46 $\pm$ 0.05 nm for the organic film and dispersion curves for the dielectric permittivities and refractive index as shown in Fig. 3. The imaginary component peaks at *ca.* 550 nm, the closest laser wavelength being 543.5 nm. Comparison with Fig. 2 shows a discrepancy, λ_{max} = 500 nm, which may arise from slightly altered packing on different substrates: gold for SPR and an adjacent organic layer for the spectrum. Furthermore, the asymmetric transition of Fig. 2 indicates separate maxima at *ca.* 480 and 560 nm, the latter almost matching that obtained from ε_i. Dispersion of the real component (ε_r) and refractive index (n) also reflect the broad visible range absorption band but a characteristic broadening

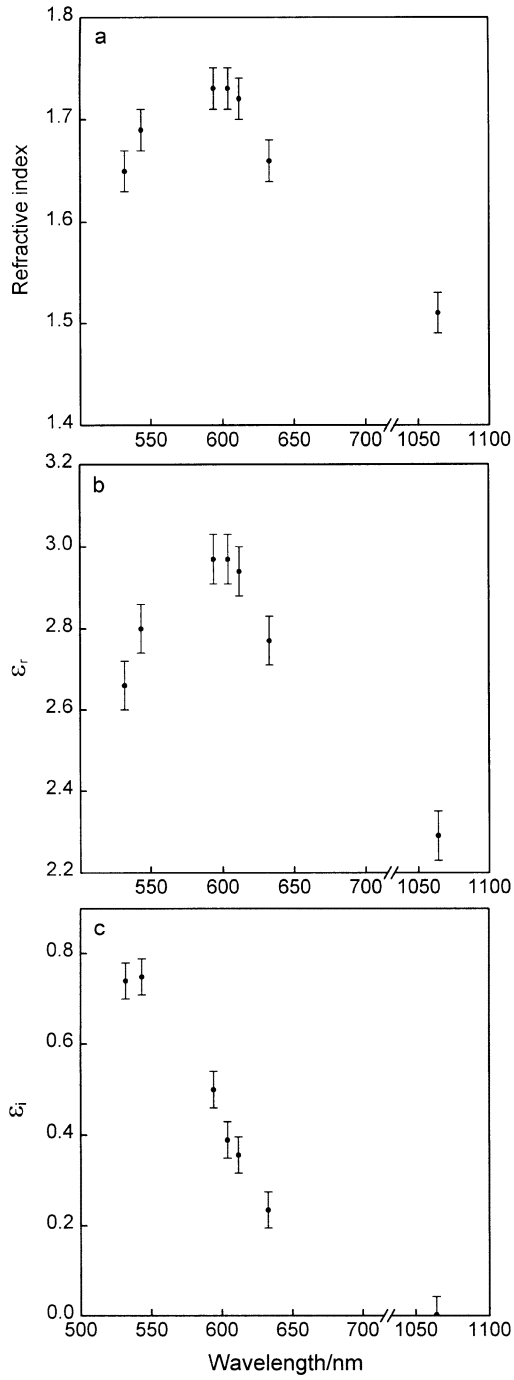

Fig. 3 Dispersion curves: (a) refractive index; (b) real component of the dielectric permittivity; (c) imaginary component.

of the SPR spectra prevents accurate analysis at excitatory laser wavelengths below that of the frequency-doubled Nd : YAG.

The dye is almost transparent above 750 nm and, thus, is more useful for second-order nonlinear optical applications at wavelengths other than 1064 nm used in this study. This is particularly relevant as the LB multilayer is one of very few[13–15] to lack inversion symmetry unless interleaved by spacer layers.[16,17] A structure of this type is rare. It is attributed in this case to the dibutylamino group being sufficiently hydrophobic to suppress realignment both during and after deposition. It contrasts with numerous amphiphilic dyes, which pack centrosymmetrically with their hydrophilic groups at one interface and hydrophobic groups at the next. The alignment in this work has been confirmed by the second-harmonic intensity, which increases quadratically with the number of layers in thin films but is affected by absorption at the harmonic wavelength as the thickness increases (Fig. 4).

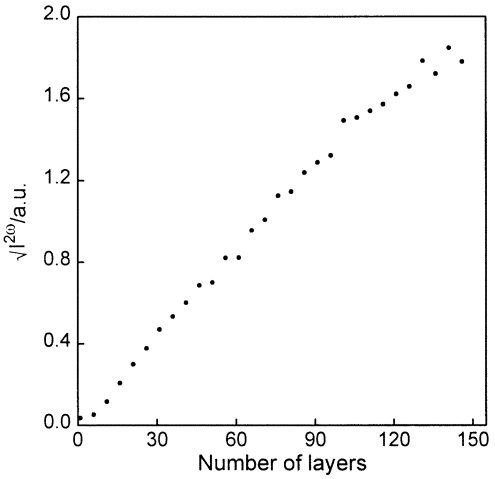

Fig. 4 Variation of the square root of the second-harmonic intensity with the number of LB layers, the intensity being measured in transmission with the laser beam (Nd : YAG, p-polarised) incident at 45° to the film.

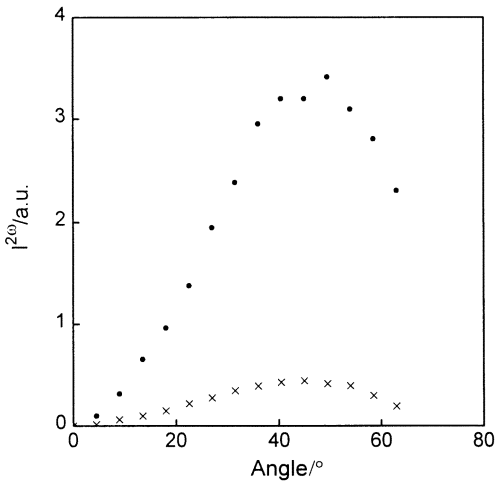

Fig. 5 Second-harmonic intensity *vs.* angle of incidence of the Nd : YAG laser beam: p-polarised (●); s-polarised (×).

The second-harmonic intensity was measured in transmission and investigated as the angle of incidence of the laser beam, relative to the LB film, was altered from 0 to 65° for both p and s polarisations (Fig. 5). The signal is negligible at normal incidence and, throughout the range, $I^{2\omega}(p \rightarrow p)$ is significantly stronger than $I^{2\omega}(s \rightarrow p)$. The polarisation dependence was also investigated as the half-wave plate was rotated at a fixed angle of incidence of the laser beam relative to the LB film (Fig. 6). From the data of Figs. 5 and 6 we estimate a chromophore tilt angle of *ca.* 45° from the normal to the substrate. Furthermore, the effective susceptibility obtained from the intensity at the optimal angle, when calibrated against the Maker fringe envelope of a Y-cut quartz reference (d_{11} = 0.5 pm V^{-1}), is typically $\chi^{(2)}_{eff}$ = 80 pm V^{-1} for the LB monolayer. The high value arises from resonant enhancement at the harmonic wavelength.

Molecular rectification

Molecular rectification has been reported for a related cationic dye[3,4] sandwiched between gold electrodes: Au/(D–π–A)/Au. At one end, electrons tunnel from the electrode to the acceptor and, at the other, from the donor to the electrode whereas, under reverse bias, tunnelling is not readily attainable because the donor is a poor electron-acceptor and the acceptor a poor electron-donor. In this work, using the quinolinium analogue of the dye, multilayer LB films were deposited onto glass

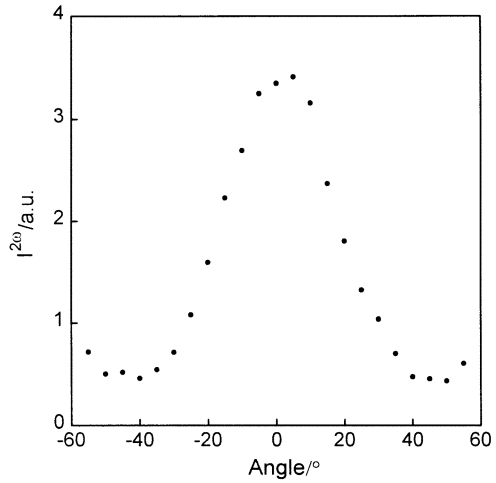

Fig. 6 Second-harmonic intensity *vs.* the rotation angle of the half-wave plate for the Nd : YAG laser incident at 45° to the film. The maximum and two minima correspond to the fundamental beam being p and s-polarised respectively.

substrates, which had been pre-coated with either gold or aluminium. Optimum alignment was confirmed by SHG studies, by having a window in the base electrode, the susceptibility being consistent in each case with that obtained above. An Edwards 306 coating unit, operating at 10^{-4} Pa, was then used to evaporate gold or aluminium pads onto the film at a rate of 0.1 nm s^{-1}.

Current–voltage curves were obtained for an Au/LB/Au structure comprising 5 LB layers and Al/LB/Al devices, with a thicker organic overlay comprising 40 LB layers (Figs. 7 and 8). The dependence is reproducible and both gave asymmetric current–voltage curves, which may be unambiguously assigned to molecular rectification for the non-oxidisable gold electrodes. With positive bias the data from both plots vary as $J \propto e^{\alpha V}$ above a small threshold voltage. Only two film thicknesses have been studied, albeit very different in the number of LB layers, but the data clearly indicate that α is proportional to the inverse of the number. Therefore, the current density increases exponentially with electric field (Fig. 9), *i.e.* as:

$$J = J_o\, e^{\beta E} \qquad (2)$$

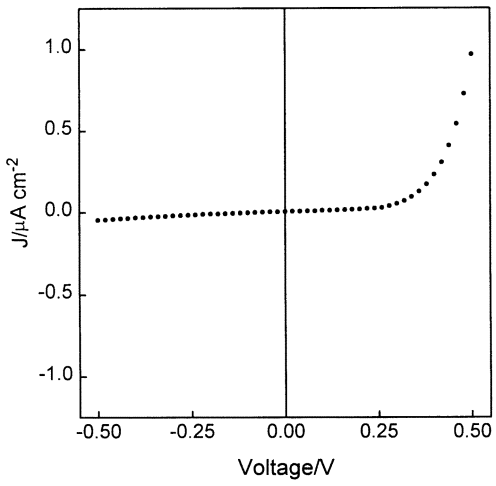

Fig. 7 Current–voltage characteristics of an Au/(LB film)/Au device obtained using a scan rate of +30 mV s^{-1} and a 5 layer LB film, the thickness being determined from the absorbance, corrected for the semi-transparent gold, following evaporation of the top electrode. The current density varies as $J \propto e^{\alpha V}$ for V greater than *ca.* 0.2 V and α = 14.8 V^{-1}. Slight hysteresis was observed for the scan in the negative direction but, for clarity, this is not shown in the figure.

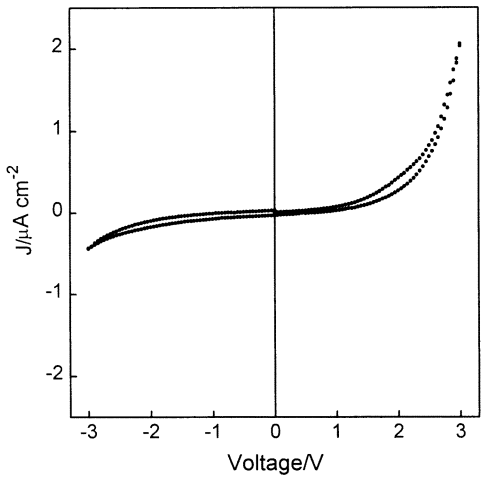

Fig. 8 Current–voltage characteristics of an Al/(LB film)/Al device obtained using a scan rate of 30 mV s^{-1}, the LB film being 40 layers prior to deposition of the top electrode. The current density varies as $J \propto e^{\alpha V}$ above a threshold voltage: α = 1.82 V^{-1} above *ca.* 0.2 V and α = 1.89 V^{-1} above *ca.* 1 V for scans in the positive and negative directions respectively. The slight hysteresis could relate to a field-induced shift of the negatively charged counterion relative to the cationic dye.[4]

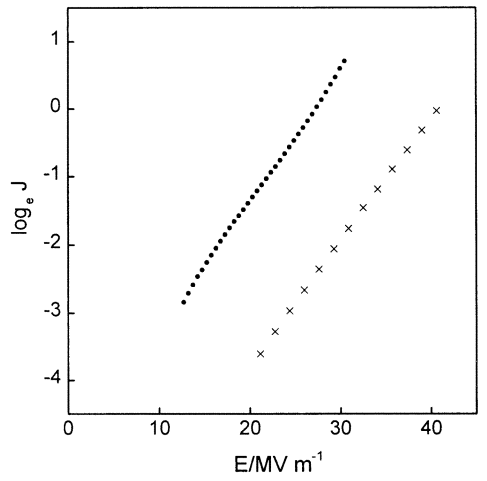

Fig. 9 Natural logarithm of the current density *vs.* electric field for device structures with different numbers of layers, Au/(5 LB layers)/Au (×) and Al/(40 LB layers)/Al (●), both with positive bias and above the threshold voltage. The data correspond to scans in the positive and negative directions respectively and the electric field to $E = V/Nd$ where N is the number of LB layers and d is the monolayer thickness determined from the SPR study.

where β^{-1} is *ca.* 5.5 MV m^{-1}, assuming a thickness of 2.46 nm $layer^{-1}$ and correct assignment of the number after evaporation of the top electrode. The pre-exponential factor, J_o, should be constant but, as the evaporated electrode is probably filamentary rather than planar, partial penetration of the fragile organic layer may cause it to vary from sample to sample.

We have found that some samples, albeit few, exhibit a weaker dependence and that the behaviour is symmetrical in the negative and positive quadrants of the current–voltage plots. Also, when the rectifying samples are cycled, the current at positive bias diminishes while that at negative bias increases until the curves became symmetrical. The behaviour is attributed here to anion induced effects and may be compared with the previously reported data obtained for 5-[4-(*N*,*N*-dibutylamino)benzylidene]-2-alkyl-5,6,7,8-tetrahydroisoquinolinium octadecyl sulfate, the cationic dye referred to in the introduction.[3,4] For this salt, there is both experimental and

Table 1 Theoretically modelled (MNDO) dimensions of 4-[2-(4-aminophenyl)vinyl]-*N*-methylquinolinium acetate, the hydrophobic group being omitted to save on computing time. The aromatic and quinonoid forms relate to molecular structures with the negatively charged counterion located adjacent to the heterocycle and amino group respectively

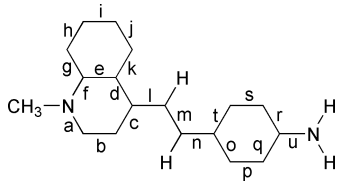

Bond	Aromatic bond length/Å	Quinonoid bond length/Å	Δ(Ar − Q)/Å
Heterocycle			
a	1.369	1.400	−0.031
b	1.409	1.368	0.041
c	1.400	1.456	−0.056
d	1.459	1.480	−0.021
e	1.436	1.437	−0.001
f	1.415	1.418	−0.003
g, k	1.439, 1.439	1.426, 1.424	0.014
h, j	1.385, 1.383	1.396, 1.397	−0.013
i	1.422	1.410	0.012
Exocyclic π-bridge			
L	1.471	1.388	0.083
m	1.358	1.434	−0.076
n	1.469	1.393	0.076
Anilino group			
o, t	1.415, 1.425	1.459, 1.460	−0.040
p, s	1.404, 1.401	1.373, 1.375	0.029
q, r	1.420, 1.410	1.453, 1.454	−0.039
u	1.418	1.357	0.061

theoretical evidence to suggest that the molecular dipole is reversed when the negatively charged counterion is shifted from the heterocycle towards the amino group:[4] *e.g.*, (a) the polarity for rectification is reversed; (b) the second-harmonic intensity is cancelled in non-centrosymmetric structures where the counterion is located at both ends; (c) the theoretically derived molecular dimensions show a distinct change in bond alternation from the aromatic form (D–π–A^+ X^-) to quinonoid form (X^- D^+=π=A). This has also been established for the chromophore reported in this work using the MOPAC programme of Cerius2 (Accelrys, Cambridge) and a molecule without hydrophobic alkyl groups to reduce the computing time. MNDO, AM1 and PM3 calculations indicate significant changes in the molecular dimensions as the counterion is shifted. These are particularly pronounced for the central exocyclic bridging unit, which has single–double–single and double–single–double configurations in the aromatic and quinonoid forms respectively, and the exocyclic C–N bond connecting the amino group (Table 1). Furthermore, when the probe charge is located towards the centre of the molecular unit, rather than at the active ends, the dimensions show minimal bond alternation, equivalent to a resonant charge-transfer state. Thus, it may be assumed that anion displacement gives rise to the symmetrical current–voltage characteristics when the rectifying structures are cycled.

Conclusion

The cationic dye shows asymmetric current–voltage curves when sandwiched as an LB film between gold or aluminium electrodes and, with positive bias, the current increases exponentially with the electric field. The asymmetry is attributed to molecular rectification but the current decreases with successive cycles, which is probably induced by the counterion. Analysis has shown that the molecular structure can alter from the conventional aromatic form (D–π–A^+ X^-) to the quinonoid form (X^- D^+=π=A) as the negatively charged counterion relocates from the quinolinium end to the amino group. This was first suggested for a related cationic dye[4] and has been established in this work by theoretical modelling.

Acknowledgement

We are grateful to the EPSRC (UK) for support of this work, including the provision of PhD studentships to D.S.G. and R.H., and acknowledge Andy Green, Sam Kelly, Anne Whittam and previously, Chris Jones and Chris George for technical assistance.

References

1 A. S. Martin, J. R. Sambles and G. J. Ashwell, *Phys. Rev. Lett.*, 1993, **70**, 218; G. J. Ashwell, J. R. Sambles, A. S. Martin, W. G. Parker and M. Szablewski, *J. Chem. Soc., Chem. Commun.*, 1990, 1374.
2 A. C. Brady, B. Hodder, A. S. Martin, J. R. Sambles, C. P. Ewels, R. Jones, P. R. Bridden, A. M. Musa, C. A. Panetta and D. L. Mattern, *J. Mater. Chem.*, 1999, **9**, 2271.
3 G. J. Ashwell and D. S. Gandolfo, *J. Mater. Chem.*, 2001, **11**, 246.
4 G. J. Ashwell and D. S. Gandolfo, *J. Mater. Chem.*, 2002, **12**, preceding paper (DOI: 10.139/b109872c).
5 A. Aviram and M. Ratner, *Chem. Phys. Lett.*, 1974, **29**, 277.
6 G. J. Ashwell, *Thin Solid Films*, 1990, **186**, 155; G. J. Ashwell, G. Jefferies, E. J. C. Dawnay, A. P. Kuczynski, D. E. Lynch, G. Yu and D. G. Bucknall, *J. Mater. Chem.*, 1995, **5**, 975.
7 R. M. Metzger, B. Chen, U. Hopfner, M. V. Lakshmikantham, D. Vuillaume, T. Kawai, X. Wu, H. Tachibana, T. V. Hughes, H. Sakurai, J. W. Baldwin, C. Hosch, M. P. Cava, L. Brehmer and G. J. Ashwell, *J. Am. Chem. Soc.*, 1997, **119**, 10455.
8 T. Xu, I. R. Peterson, M. V. Lakshmikantham and R. M. Metzger, *Angew. Chem., Int. Ed.*, 2001, **40**, 1749.
9 G. J. Ashwell and G. A. N. Paxton, *Aust. J. Chem.*, in press.
10 G. Sauerbrey, *Z. Phys.*, 1959, **155**, 206.
11 G. J. Ashwell, A. J. Whittam, M. A. Amiri, R. Hamilton, A. Green and U. W. Grummt, *J. Mater. Chem.*, 2001, **11**, 1345.
12 E. Kretschmann, *Z. Phys.*, 1971, **241**, 313.
13 G. J. Ashwell, *J. Mater. Chem.*, 1999, **9**, 1991 (Feature Article).
14 G. J. Ashwell, P. D. Jackson and W. A. Crossland, *Nature*, 1994, **368**, 438; G. J. Ashwell, R. Ranjan, A. J. Whittam and D. Gandolfo, *J. Mater. Chem.*, 2000, **10**, 63; G. J. Ashwell, R. Hamilton, B. J. Wood, I. R. Gentle and D. Zhou, *J. Mater. Chem.*, 2001, **11**, 2966.
15 G. Decher, B. Tieke, C. Bosshard and P. Günter, *Ferroelectrics*, 1989, **91**, 193.
16 S. H. Ma, X. Z. Lu, J. H. Xu, W. C. Wang and Z. M. Zhang, *J. Phys. D*, 1997, **30**, 2651.
17 W. M. K. P. Wijekoon, S. K. Wijaya, J. D. Bhawalkar, P. N. Prasad, T. L. Penner, N. J. Armstrong, M. C. Ezenyilimba and D. J. Williams, *J. Am. Chem. Soc.*, 1996, **118**, 4480.